

Original Research Communication

Mitochondrial Control of Inducible Nitric Oxide Production in Stimulated RAW 264.7 Macrophages

OREN TIROSH,¹ QIONG GUO,² CHANDAN K. SEN,³ and LESTER PACKER²

ABSTRACT

Addition of glucose to activated RAW 264.7 macrophages or addition of mitochondrial electron-transfer chain inhibitors enhanced the cellular nitric oxide production. An additive effect of rotenone or antimycin A and glucose on enhancing nitric oxide production was shown. Uncoupling the mitochondria by a chemical uncoupler decreased nitric oxide production. The mitochondria membrane potential was found to be important for cell viability. Although nitric oxide is the physiological inhibitor of mitochondrial respiration, this study indicates that mitochondria were not inhibited in the activated macrophages. Furthermore, a role of mitochondria in the rapid regulation of nitric oxide synthesis by the inducible nitric oxide synthase has been demonstrated. *Antioxid. Redox Signal.* 3, 711–719.

INTRODUCTION

DIFFERENT KINDS OF IMMUNE STIMULI to inflammatory cells promote the expression of the cytosolic inducible nitric oxide synthase (iNOS). Such signal transduction-dependent gene expression of iNOS facilitates the commitment of a macrophage for its antitumor and cytotoxic activity (10, 14). At normal cellular calcium levels nitric oxide (NO[•]) production by iNOS is believed to be limited only by the amount of enzyme substrates or cofactors present. This hypothesis has been demonstrated by the addition of L-arginine to stimulated immune cells (1, 3). However, little is known whether changes in other iNOS co-factors such as pyridine nucleotides level in cells and

whether the cellular energetic status can regulate NO[•] production.

NO[•] is so far the only known physiological inhibitor of mitochondrial respiration (4, 21). This regulatory effect is facilitated by two separate mechanisms: (a) NO[•] can inhibit reversibly at low physiological concentrations the mitochondrial respiration (4, 21), and (b) in contrast, peroxynitrite, a product of NO[•] reaction with superoxide radical (2), causes irreversible inhibition of mitochondrial respiration, which is accompanied by extensive protein oxidation and lipid peroxidation (7, 18). The binding site of NO[•] to mitochondria is primarily the oxygen-binding site of the cytochrome oxidase (22, 23). Such an interaction results in the inhibition of the electron respira-

¹Institute of Biochemistry, Food Science and Nutrition, The Hebrew University of Jerusalem, Rehovot 76100, Israel.

²Department of Molecular Pharmacology and Toxicology, School of Pharmacy, University of Southern California, 1985 Zonal Avenue, Los Angeles, CA 90089-9121, U.S.A.

³Laboratory of Molecular Medicine, The Ohio State University Medical Center, Columbus, OH 43210, U.S.A.

tory chain in the mitochondria and cellular oxygen consumption. A low level of NO \cdot caused significant reversible inhibition of the mitochondrial respiration dependent on the oxygen tension (5).

In this study we have used electron spin resonance (ESR) and spin-trapping techniques (12, 17, 25) to test the hypothesis that NO \cdot production in RAW 264.7 macrophages stimulated by interferon- γ (IFN- γ) and lipopolysaccharide (LPS) (11, 24) is regulated by the cell metabolism and by the degree of mitochondrial energetic status. We have demonstrated that (a) macrophages up-regulate reduced pyridine nucleotides within minutes in response to glucose or by treatment with mitochondria respiration inhibitors, which results in multifold enhanced production of NO \cdot , (b) RAW 264.7 macrophages maintain mitochondrial respiratory chain activity in spite of the NO \cdot -generated flux, and (c) the mitochondrial membrane potential is vital for the activated macrophages to sustain viability.

MATERIALS AND METHODS

Materials

Sodium *N*-methyl-D-glucamine dithiocarbamate (MGD) was from Polyscience Inc. (War-rington, PA, U.S.A.). *L*-Lysine, *N*^G-monomethyl-*L*-arginine (*L*-NMMA), superoxide dismutase (SOD), *L*-arginine, rotenone, carbonyl cyanide *p*-trifluoromethoxyphenylhydrazine (FCCP), and antimycin A were from Sigma (St. Louis, MO, U.S.A.). Propidium iodide (PI) and 5,5',6,6'-tetra-chloro-1,1',3,3'-tetraethylbenzimidazolylcarbo-cyanine iodide (JC-1) were from Molecular Probes (Eugene, OR, U.S.A.). RPMI 1640 medium and Dulbecco's phosphate-buffered saline (DPBS) were obtained from GIBCO (Gaithersburg, MD, U.S.A.). IFN- γ and LPS were purchased from Genzyme (Cambridge, MA, U.S.A.). Fetal calf serum was obtained from the University of California, San Francisco cell culture facility.

Iron-dithiocarbamate complex spin trap agent [(MGD) $_2$ -Fe $^{2+}$] for trapping NO \cdot was prepared by reacting MGD (25 mM) with FeSO $_4$ (5 mM).

The FeSO $_4$ solution was freshly prepared for each experiment (17).

Cell culture

The murine cell line of monocyte macrophages RAW 264.7 (American Type Culture Collection, Rockville, MD, U.S.A.) was used in this study to generate NO \cdot (11). Cells were grown at 37°C 5% CO $_2$ in RPMI 1640 medium supplemented with 10% fetal calf serum, 1% (wt/vol) penicillin-streptomycin, and 2 mM *L*-glutamine. Cells were utilized for experiments at ~90% confluence.

Experimental design: production of NO \cdot in stimulated cells

RAW 264.7 cells were stimulated for 6 h with 10 μ g/ml LPS and 50 units/ml IFN- γ . Cells in monolayer were washed twice with DPBS (room temperature) and then harvested. Cells were spun down, the DPBS was aspirated, and cells were resuspended in DPBS; cells were then counted and aliquots taken for the experiment. *L*-Arginine, glucose, mitochondrial respiration regulators, and the spin trap complex [(MGD) $_2$ -Fe $^{2+}$] were added to the stimulated cells. The strategy was to avoid interference of the glucose and mitochondrial regulators with iNOS expression during activation. The mixture was incubated in a water bath at 37°C for 90 min, and then the entire sample was loaded into a quartz glass flat cell for ESR measurement. Each sample contained 2.4×10^6 cells in a final volume of 75 μ l. Rotenone, antimycin A, and FCCP were dissolved in dimethyl sulfoxide (DMSO) concentrations so that the final concentration of the solvent in cell culture suspension did not exceed 0.2% (vol/vol). Respective controls were treated with an equal volume of DMSO.

Electron spin resonance spectroscopy

ESR spectra were recorded using an IBM ER 200D-SRC ESR spectrometer (Danbury, CT, U.S.A.). The following ESR spectroscopy settings were used: central field, 3420 G; modulation frequency, 100 kHz; modulation amplitude, 3.2 G; microwave power, 20 mW; scan

width, 200 G; gain, 6.3×10^5 ; temperature, 298K.

Griess reaction assay of nitrite formation from stimulated macrophages

The amount of nitrite production in the incubation medium was determined by using the Griess reaction (6, 13). The Griess reaction was carried out to quantify the total nitrite production (nitrite plus nitrate) occurring during the period of incubation using a NO[•] assay kit. In brief, after a 90-min incubation, the incubation medium was centrifuged and supernatants were collected and mixed for 20 min with nitrate reductase and NADH, which were used to convert the nitrate to nitrite prior to quantification using the Griess assay; then the Griess reagent [1% sulfanilamide/0.1% *N*-(1-naphthyl)ethylenediamine dihydrochloride in 3 M HCl] was added and the mixture incubated for 10 min at room temperature. The total nitrite concentration was determined by measuring the absorbance at 540 nm in a Titertek Multiskan (Flow Laboratories, North Ryde, Australia). Total nitrite concentration was calculated using potassium nitrite as a standard.

Determination of cell viability

Cell membrane integrity was detected by flow cytometry (EPICS Elite or XL, Coulter, Miami, FL, U.S.A.) as a measurement of cell viability. For this assay, the nonpermeant DNA interchelating dye PI, which is excluded by viable cells, was used. Fluorescence settings were excitation at 488 nm and emission at 575 nm (20).

Measurement of intracellular NAD(P)H content using flow cytometer

Over 90% of the cellular autofluorescence is accounted for by reduced pyridine nucleotides (16). Therefore, after a 6-h stimulation with LPS and IFN- γ , macrophages were harvested in DPBS and treated in the presence of 0.7 mM L-arginine with 5 μ M rotenone, 5 μ g/ml antimycin A, or 25 mM glucose. Then aliquots were taken from the cell suspension at different time points and analyzed by flow cytome-

ter (EPICS Elite or XL). Cells were excited with a blue laser at 340 nm and detected between 400 and 480 nm. A mean autofluorescence of 10,000 viable cells per sample was collected (9).

Determination of mitochondrial membrane potential (MMP)

Determination of MMP was carried out using the ratiometric dye JC-1, a dual-emission potential-sensitive probe. The green fluorescent (emission at 529 nm) JC-1 exists as a monomer at low concentrations or at low membrane potential. However, at higher concentrations (aqueous solutions above 0.1 μ M) JC-1 forms red fluorescent "J-aggregates" that exhibit a broad excitation spectrum and an emission maximum at \sim 590 nm. To stain cells with JC-1, 2.4×10^6 cells (75 μ l) were resuspended in 0.5 ml of DPBS containing 2.5% bovine serum albumin and incubated with 10 μ g/ml JC-1 for 15 min at room temperature. The cells were then diluted 100 times by DPBS and analyzed by flow cytometer.

Statistical analysis

Statistical analysis was carried out by analysis of variance. $p < 0.05$ was considered significant. Experimental data are expressed as the means of three experiments \pm SD.

RESULTS

NO[•] production from macrophages

Introduction of a spin-trap agent, the [(MGD)₂-Fe²⁺] complex, to activated macrophages in the presence of 0.7 mM L-arginine produced a three-line ESR spectrum of the [(MGD)₂-Fe²⁺-NO] spin adduct (Fig. 1A). The spectral parameters of this ESR signal ($g = 2.04$, $a^N = 12.5$ G) are identical to those reported in the literature when an aqueous solution of authentic NO[•] was added to a solution containing the complex of iron and MGD (21).

Activation of cells with a combination treatment of IFN- γ plus LPS resulted in NO[•] production as was detected by ESR. NO[•] signals were detectable and peaked after 4 and 6 h of

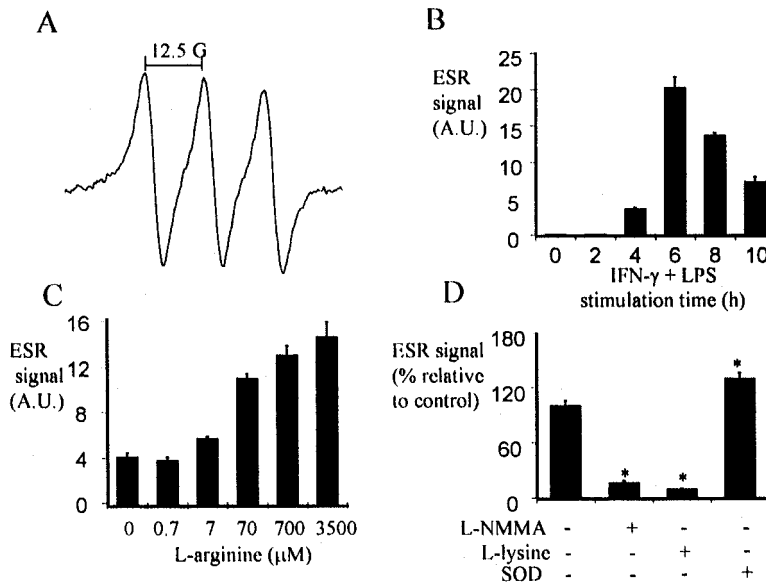


FIG. 1. ESR detection of NO \cdot production from RAW 264.7 macrophages. Cells were activated with 50 units/ml IFN- γ and 10 μ g/ml LPS, and then cells were harvested in DPBS and incubated in the presence of the spin-trap agent (MGD) $_2$ -Fe $^{2+}$ with the iNOS substrate L-arginine for 90 min. Cells were then loaded for ESR measurement (see Materials and Methods). (A) A typical ESR spectrum of the (MGD) $_2$ -Fe $^{2+}$ -NO spin adduct. (B) Effect of time-dependent exposure of cells to IFN- γ and LPS on the NO \cdot production in the presence of 0.7 mM L-arginine. (C) Effect of increasing concentrations of L-arginine on NO \cdot production from cells that were activated by IFN- γ and LPS for 6 h. (D) Effect of L-NMMA (0.1 mM), L-lysine (5.0 mM), or SOD (50 units/ml) on NO \cdot production from 6-h-stimulated cells in the presence of 0.7 mM L-arginine. Data are normalized to the control. * $p < 0.05$, different compared with control.

activation, respectively. Further exposure resulted in a weaker ESR signal, indicating diminished NO \cdot production (Fig. 1B). Therefore, all other experiments were carried out using 6-h activated cells. The dependency of NO \cdot formation on the presence of the iNOS substrate, L-arginine, was studied by incubating activated macrophages for 90 min in the presence of increasing concentrations of L-arginine (0–3.5 mM). L-arginine induced a marked increase in NO \cdot production up to 0.7 mM. Higher concentrations of L-arginine resulted in only a minor further increase in NO \cdot production (Fig. 1C). Inhibition of the ESR signal in the presence of 0.7 mM L-arginine has been facilitated by using the iNOS inhibitor L-NMMA and by using L-lysine as an L-arginine uptake competitor. SOD increased the NO \cdot signal by 30% (Fig. 1D).

Glucose and mitochondrial regulation of NO \cdot production

NO \cdot production from cells was markedly affected by glucose. The addition of glucose to the activated cell suspension in the presence of L-arginine showed up to threefold increase in

the NO \cdot production (Fig. 2). The enhancement effect of glucose on NO \cdot production was saturated at 2.5 mM glucose, and further supplementation with up to 25.0 mM glucose did not show further augmentation (Fig. 2).

Cells treated with a 5 μ M concentration of the mitochondrial complex I inhibitor rotenone showed a marked increase in NO \cdot production (Fig. 3). Rotenone also exacerbated the effect of glucose. Antimycin A, another inhibitor of the

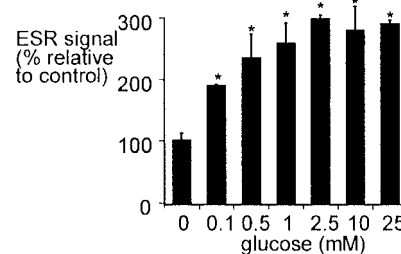


FIG. 2. Glucose-induced increase in NO \cdot production from cells. Activated cells (2.4×10^6) in the presence of 0.7 mM L-arginine were treated with different concentrations of glucose for 90 min (see Materials and Methods). NO \cdot release was then evaluated by ESR signal. * $p < 0.05$, higher compared with L-arginine-treated control.

mitochondrial electron transfer chain (ETC; complex III inhibitor), was used to confirm the effect of mitochondrial respiration inhibition on NO[•] production. Cells treated with 5 μg/ml antimycin A showed a marked increase in NO[•] production. Additive effects of rotenone or antimycin A and glucose on NO[•] production have been shown (Fig. 3).

Rotenone as a complex I inhibitor and antimycin A as a complex III inhibitor deenergized mitochondria and diminished the MMP. To evaluate the role of MMP on NO[•] production and cell viability, FCCP, a mitochondrial uncoupler that has no inhibitory effect on the mitochondrial ETC was used. FCCP decreased the NO[•] production by 20–30% from cells both alone and in the presence of glucose (Fig. 4). As FCCP, antimycin A, and rotenone had similar toxic effects to the cells as was measured by PI exclusion assay (Fig. 5A) and had similar reflection on cell size (Fig. 5B), it can be concluded that only specific inhibition of the ETC facilitated NO[•] production, whereas its acceleration by mitochondrial uncoupling decreased NO[•] production. Glucose had a stupendous effect on improving the cell condition as was evaluated from the flow cytometry PI exclusion data and forward scatter measurements of cell size (Fig. 5).

Griess reaction assay: total nitrite accumulation

Indirect measurements of NO[•] production from macrophages by the colorimetric Griess

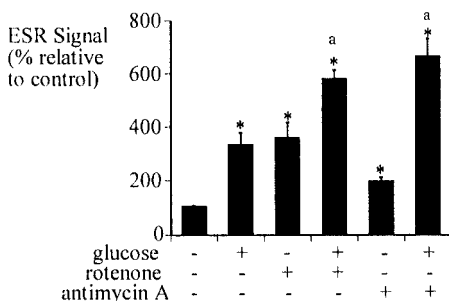


FIG. 3. Exacerbating effect of mitochondrial respiratory chain inhibitors on NO[•] production from cells. Activated cells (2.4×10^6) in the presence of 0.7 mM L-arginine were treated with 5 μM rotenone or 5 μg/ml antimycin A in the presence or absence of 25 mM glucose for 90 min. NO[•] release was then evaluated by ESR signal. * $p < 0.05$, higher compared with L-arginine-treated control. ^a $p < 0.05$, higher compared with the corresponding glucose-treated control.

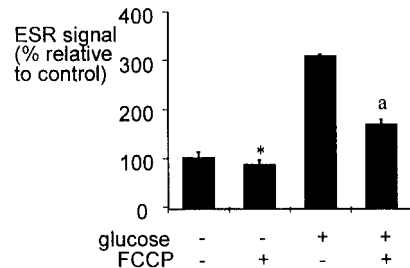


FIG. 4. Inhibitory effect of the mitochondrial uncoupler FCCP on NO[•] production from cells. Activated cells (2.4×10^6) in the presence of 0.7 mM L-arginine were treated with 10 μM FCCP in the presence or absence of 25 mM glucose for 90 min. NO[•] release was then evaluated by ESR signal. * $p < 0.05$, lower compared with L-arginine-treated control. ^a $p < 0.05$, lower compared with the corresponding glucose-treated control.

reaction assay for total nitrite accumulation showed a basal production in the presence of 0.7 mM L-arginine of 156 ± 20 pmol/ 10^6 cells/h. This production rate provided a total nitrite concentration of 7.5 μM after 90 min of incubation. The mitochondria ETC inhibitors rotenone and antimycin A elevated the total nitrite accumulation by 30% (data not shown).

MMP in activated macrophages

Treatment of activated cells with L-arginine resulted in some loss of MMP (Table 1) as determined by the red fluorescence component (J-aggregate) of the membrane potential-sensitive dye JC-1. Rotenone or antimycin A treatment further obliterated the MMP. However, glucose treatment induced an extensive elevation in MMP.

Cellular reduced pyridine nucleotide level

Changes in the cellular NAD(P)H levels are shown in Fig. 6. Treatment of macrophages with glucose, rotenone, or antimycin A enhanced the NAD(P)H level. Glucose, rotenone, or antimycin A up-regulated the cellular reduced pyridine nucleotide NAD(P)H level within 10 min of incubation. Therefore, the mitochondrial ETC in immune stimulated macrophages functions as a consumption pathway for cellular reduced pyridine nucleotides.

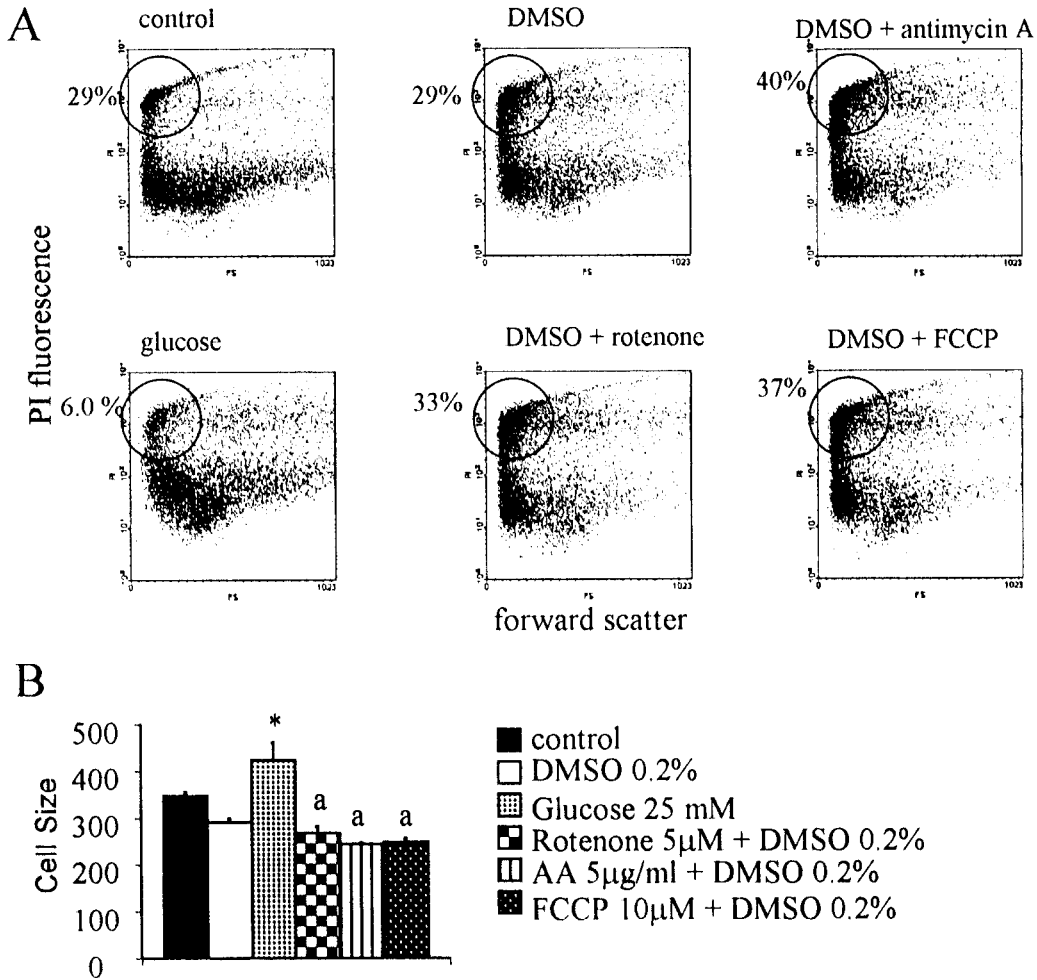


FIG. 5. Cell viability. (A) Flow cytometer dot plot presentations of 10,000 cells incubated with 2 μ g/ml PI in DPBS: control cells, 25 mM glucose-treated cells, DMSO (0.2%)-treated cells, DMSO + rotenone (5 μ M), DMSO + antimycin A (AA) (5 μ g/ml), DMSO + FCCP (10 μ M). The numbers on the left side of the plots represent percentage of dead cells. (B) Mean cell size measured by forward scatter. * $p < 0.05$, higher compared with control. ^a $p < 0.05$, lower compared with DMSO-treated control.

DISCUSSION

Production of NO \cdot from an NOS can be up-regulated in immune-system cells (5, 15). As NO \cdot is the physiological mitochondrial respiration inhibitor, it was of interest to evaluate the reciprocal interactions between mitochondria and NO \cdot in inflammatory cells.

Mitochondrial ETC is not inhibited in activated macrophages

Inhibition of the mitochondrial ETC by two different inhibitors, rotenone and antimycin A, resulted in enhanced production of NO \cdot , whereas the mitochondrial uncoupler that accelerates mitochondrial respiration decreased

TABLE 1. CHANGES IN MMP IN ACTIVATED MACROPHAGES

JC-1	Control	L-Arginine	L-Arginine + glucose	L-Arginine + rotenone	L-Arginine + AA
J-aggregates (FL2 fluorescence)	1.00 \pm 0.05	0.92 \pm 0.09	1.67 \pm 0.04*	0.82 \pm 0.01*	0.81 \pm 0.05*

Macrophages were treated or not with 0.7 mM L-arginine, 25 mM glucose, 5 μ g/ml antimycin A (AA), or 5 μ M rotenone for 90 min in DPBS. Cells were then stained with the dye JC-1.

* $p < 0.05$, different compared with control value.

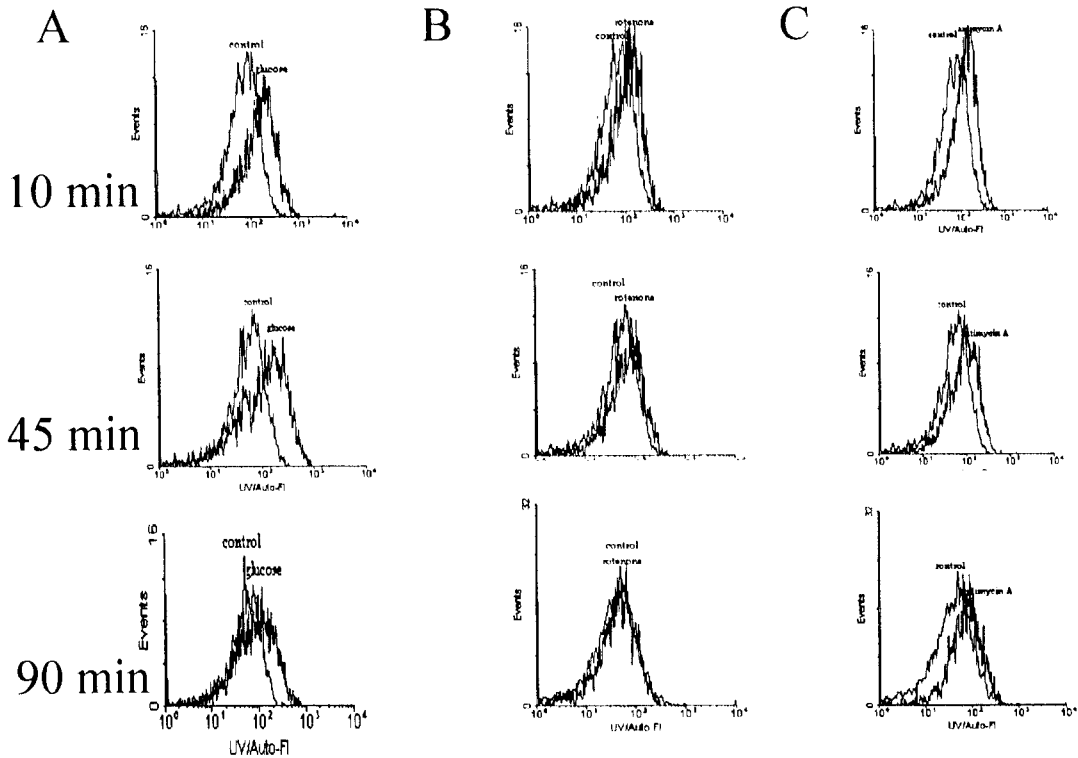


FIG. 6. Regulation of intracellular NAD(P)H concentrations. Activated cells (2.4×10^6) in the presence of 0.7 mM L-arginine were diluted 100 times with DPBS after treatments. The panels show flow cytometer histograms representing changes in cell autofluorescence (340 nm) of 5,000 cells (A) with and without glucose (25 mM), (B) with and without rotenone (5 μ M) and (C) with and without antimycin A (5 μ g/ml).

NO[•] production. This line of evidence suggests that the ETC of mitochondria of activated RAW 264.7 macrophages were not blocked by the high amount of NO[•] released. Supporting evidence includes the elevation in membrane potential in response to glucose and the fast elevation in reduced pyridine nucleotide content of the cells following rotenone or antimycin A treatment. These data indicate that the ETC in the macrophages were effectively excluding protons from the mitochondria matrix and consuming cellular reduced pyridine nucleotides. A nanomolar range of NO[•] is sufficient to block ETC completely at an atmospheric oxygen tension (5). However, the study suggests that in active macrophages that release a constant flux of NO[•] there was little or no ETC inhibition. We, therefore, hypothesize that NO[•] production is a facilitated process of releasing to the extracellular environment rather than a random leakage to the surrounding environment. Supporting the hypothesis is the combination of glucose and mitochondrial respiration inhibitors that led to an additive effect in NO[•]

production. Indicating that, the ETC in the cells were not blocked by the extensive NO[•] production instigated by glucose.

Mechanism for metabolic regulation of NO[•] production

The additive potentiation of rotenone or antimycin A with glucose was up to eightfold compared with the basal NO[•] production. The inducible enzyme has a pivotal role in the immune system function. NO[•] is needed for the cytotoxic activity during pathological situations, *e.g.*, inflammation, septic shock, atherosclerosis, and cancer cell elimination (10, 14, 19). The results indicate that iNOS expression could be only an initial player in the biological response of NO[•] production.

We propose that mitochondria can regulate NAD(P)H concentrations in the vicinity of the cytosolic iNOS. Rotenone and antimycin A as two separate mitochondrial respiration inhibitors can spare NADH and diminish oxygen consumption, and therefore intensify the NO[•]

production. Introducing FCCP to cells decreased the NO[•] production. FCCP, which relieves mitochondria coupling, accelerates consumption of pyridine nucleotides by the respiratory chain. Thereby, the cellular energetic status regulates the biological specific function of NO[•] production.

Cell viability: the role of MMP

Rotenone and antimycin A collapsed the MMP by blocking the ETC, therefore abrogating the driving power for matrix-inter membrane space proton pumping. FCCP can collapse the MMP by directly delivering protons into the matrix and has been shown to do so in numerous mitochondria cell studies. A resulting of the loss of MMP is a rapid loss of cell viability. Therefore, the MMP is necessary for survival of the activated macrophages and probably cannot be self-inhibited by NO[•] which will lead to cell death and impairment of the immune response.

In conclusion, previous reports demonstrated NO[•] dependent inhibition of the mitochondrial ETC. However, a novel function of mitochondrial metabolism to down-regulate inducible NO[•] production has now been shown. Addition of glucose to macrophages was found to increase NO[•] production from activated cells at physiologically relevant concentrations. Collapsing the MMP induced rapid loss of cell viability. Therefore, mitochondria in activated macrophages modulate the immune response because they are functional and uninhibited and changes in their energetic status serve as a rapid response mechanism that regulates NO[•] production.

ACKNOWLEDGMENTS

The research was supported by NIH grant DK 50430. O.T. and Q.G. equally contributed to this work. The authors thank Drs. H. Moini and G. Rimbach for helpful discussions.

ABBREVIATIONS

DMSO, dimethyl sulfoxide; DPBS, Dulbecco's phosphate-buffered saline; ESR, electron spin

resonance; ETC, electron-transfer chain; FCCP, carbonyl cyanide *p*-trifluoromethoxyphenylhydrazine; IFN- γ , interferon- γ ; iNOS, inducible nitric oxide synthase; JC-1, 5,5',6,6'-tetrachloro-1,1',3,3'-tetraethylbenzimidazolylcarbocyanine iodide; LPS, lipopolysaccharides; MGD, sodium *N*-methyl-D-glucamine dithiocarbamate; MMP, mitochondrial membrane potential; L-NMMA, N^G-monomethyl-L-arginine; NO[•], nitric oxide; PI, propidium iodide; SOD, superoxide dismutase.

REFERENCES

1. Baydoun AR, Bogle RG, Pearson JD, and Mann GE. Arginine uptake and metabolism in cultured murine macrophages. *Agents Actions* 38: C127–C129, 1993.
2. Beckman JS and Koppenol WH. Nitric oxide, superoxide, and peroxynitrite: the good, the bad, and ugly. *Am J Physiol* 271: C1424–C1437, 1996.
3. Bogle RG, Baydoun AR, Pearson JD, Moncada S, and Mann GE. L-Arginine transport is increased in macrophages generating nitric oxide. *Biochem J* 284: 15–18, 1992.
4. Brown GC. Nitric oxide regulates mitochondrial respiration and cell functions by inhibiting cytochrome oxidase. *FEBS Lett* 369:136–139, 1995.
5. Brown GC. Nitric oxide and mitochondrial respiration. *Biochim Biophys Acta* 1411: 351–369, 1999.
6. Eigler A, Moeller J, and Endres S. Exogenous and endogenous nitric oxide attenuates tumor necrosis factor synthesis in the murine macrophage cell line RAW 264.7. *J Immunol* 154: 4048–4054, 1995.
7. Gadelha FR, Thomson L, Fagian MM, Costa AD, Radi R, and Vercesi AE. Ca²⁺-independent permeabilization of the inner mitochondrial membrane by peroxynitrite is mediated by membrane protein thiol cross-linking and lipid peroxidation. *Arch Biochem Biophys* 345: 243–250, 1997.
8. Gao JJ, Zuvanich EG, Xue Q, Horn DL, Silverstein R, and Morrison DC. Cutting edge: bacterial DNA and LPS act in synergy in inducing nitric oxide production in RAW 264.7 macrophages. *J Immunol* 163: 4095–4099, 1999.
9. Goossens V, Stange G, Moens K, Pipeleers D, and Grooten J. Regulation of tumor necrosis factor-induced, mitochondria- and reactive oxygen species-dependent cell death by electron flux through the electron transport chain complex I. *Antioxid Redox Signal* 1: 285–295, 1999.
10. Klostergaard J. Macrophage tumoricidal mechanisms. *Res Immunol* 144: 274–276, 1993.
11. Kobuchi H, Droy-Lefaix MT, Christen Y, and Packer L. Ginkgo biloba extract (EGb 761): inhibitory effect on nitric oxide production in the macrophage cell line RAW 264.7. *Biochem Pharmacol* 53: 897–903, 1997.
12. Lai CS and Komarov AM. Spin trapping of nitric ox-

- ide produced in vivo in septic-shock mice. *FEBS Lett* 345: 120–124, 1994.
13. Lancaster JR Jr and Hibbs JB Jr. EPR demonstration of iron-nitrosyl complex formation by cytotoxic activated macrophages. *Proc Natl Acad Sci U S A* 87: 1223–1227, 1990.
 14. Lorsbach RB, Murphy WJ, Lowenstein CJ, Snyder SH, and Russell SW. Expression of the nitric oxide synthase gene in mouse macrophages activated for tumor cell killing. Molecular basis for the synergy between interferon-gamma and lipopolysaccharide. *J Biol Chem* 268: 1908–1913, 1993.
 15. Murphy MP. Nitric oxide and cell death. *Biochim Biophys Acta* 1411: 401–414, 1999.
 16. Nieminen AL, Byrne AM, Herman B, and Lemasters JJ. Mitochondrial permeability transition in hepatocytes induced by *t*-BuOOH: NAD(P)H and reactive oxygen species. *Am J Physiol* 272: C1286–C1294, 1997.
 17. Norby SW, Weyhenmeyer JA, and Clarkson RB. Stimulation and inhibition of nitric oxide production in macrophages and neural cells as observed by spin trapping. *Free Radic Biol Med* 22: 1–9, 1997.
 18. Radi R, Rodriguez M, Castro L, and Telleri R. Inhibition of mitochondrial electron transport by peroxynitrite. *Arch Biochem Biophys* 308: 89–95, 1994.
 19. Schmidt HH and Walter U. NO at work. *Cell* 78: 919–925, 1994.
 20. Sen CK, Roy S, and Packer L. Fas mediated apoptosis of human Jurkat T-cells: intracellular events and potentiation by redox-active alpha-lipoic acid. *Cell Death Differ* 6: 481–491, 1999.
 21. Shen W, Hintze TH, and Wolin MS. Nitric oxide. An important signaling mechanism between vascular endothelium and parenchymal cells in the regulation of oxygen consumption. *Circulation* 92: 3505–3512, 1995.
 22. Stevens TH, Bocian DF, and Chan SI. EPR studies of ¹⁵NO-ferrocycytochrome alpha3 in cytochrome *c* oxidase. *FEBS Lett* 97: 314–316, 1979.
 23. Stevens TH, Brudvig GW, Bocian DF, and Chan SI. Structure of cytochrome a3-Cua3 couple in cytochrome *c* oxidase as revealed by nitric oxide binding studies. *Proc Natl Acad Sci U S A* 76: 3320–3324, 1979.
 24. Virgili F, Kobuchi H, and Packer L. Procyanidins extracted from *Pinus maritima* (Pycnogenol): scavengers of free radical species and modulators of nitrogen monoxide metabolism in activated murine RAW 264.7 macrophages. *Free Radic Biol Med* 24: 1120–1129, 1998.
 25. Xia Y, Dawson VL, Dawson TM, Snyder SH, and Zweier JL. Nitric oxide synthase generates superoxide and nitric oxide in arginine-depleted cells leading to peroxynitrite-mediated cellular injury. *Proc Natl Acad Sci U S A* 93: 6770–6774, 1996.

Address reprint requests to:

Dr. Oren Tirosh
Institute of Biochemistry, Food Science and
Nutrition
The Hebrew University of Jerusalem
Rehovot 76100, Israel

E-mail: orentirosh@hotmail.com

Received for publication January 12, 2001; accepted March 20, 2001.